Algorithm Theoretical Basis Document of CAPCOM for GCOM/SLGI

PI: Takashi Y. Nakajima (Tokai University TRIC)

Associate Scientist: Husi Letu (Tokai University TRIC)

2011/09/20

Table of Contents

1. Adaptation to the retrieval algorithm (CAPCOM)

CAPCOM is acronyms of Comprehensive Analysis Program for Cloud Optical Measurement. The CAPCOM uses LUT (Look up Table)-Iteration Method (LIM) to retrieve the target geophysical parameters from satellite-derived radiance data. In the CAPCOM, a non-absorption band (Band 14), an absorption band (Band 16,17), and a thermal band (Band 18) are used to derive cloud optical thickness (CLOP), cloud effective particle radius (CLER), and cloud top temperature (CLTT) (Fig. 1). Adding to these radiance data, some ancillary input data, such as the vertical profile of the temperature, pressure, water vapor, ground albedo are also used to calculate related geophysical parameters; cloud top height (CLHT) and cloud top pressure (CLTP) are retrieved by comparing cloud top temperature and temperature profile from ancillary data; liquid water path (CLWP) is calculated by cloud optical thickness and effective particle radius.

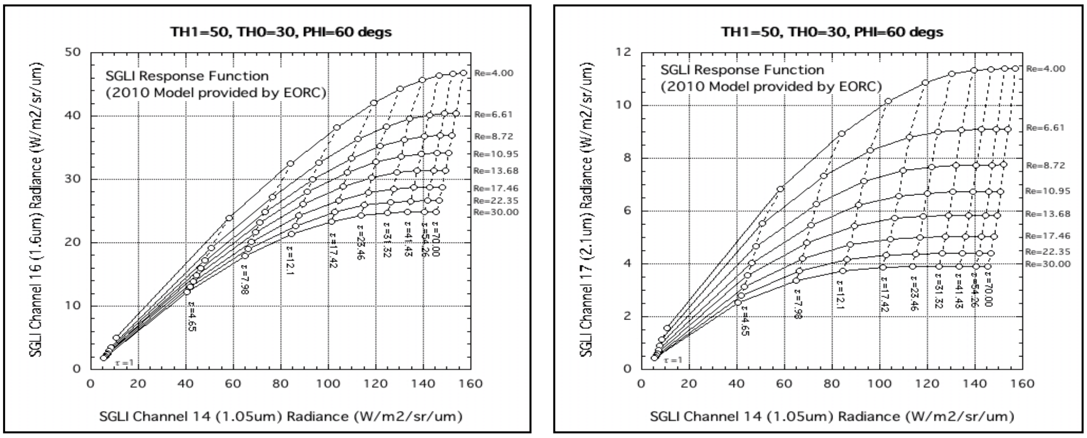

Fig. 1: Look up table for simulation of reflected solar radiances in SGLI channels

(1.05 μ m vs 1.6 μ m and 1.05μm vs 2.1 μ m)

2. Logic Flow

Four LUTs are prepared for this purpose, i. e., LUT of cloud-reflected radiance in bands 14 and 16, transmissivities and reflectivity in bands 14 and 17, band 18 transmissivity. Table 1 summarizes the grid system of the LUTs and Fig. 2 illustrates the flow of the analysis. We used Newton-Raphson method to iterate a main loop in the program. Some related parameters, such as; cloud liquid water path and cloud top height are also calculated in the CAPCOM with temperature slicing data from objective analysis such as JMA GANAL dataset. We found that the iteration does not converge in some cases of optically thin clouds when the removed radiation significantly dominates over the signal. In this case we cancel the analysis.

Table 1. The grid system of the look up tables; θ, θ_0, ϕ are the satellite and solar zenith angle, and relative azimuth angle. τ_c and r_e are cloud optical thickness and effective particle radius.

Quantities	*Grid point values*
θ(degrees)	0, 5, 10, 20, 30, 35, 50, 45, 50, 55, 60
θ_0 (degrees)	0, 5, 10, 20, 30, 35, 50, 45, 50, 55, 60, 65, 70
ϕ(degrees)	0 to 180 (divided by every 10 degrees)
τ_c (Water cloud)	1., 5., 8., 12., 17., 23., 31., 41., 54., 70
τ_c (Ice cloud)	0.1,0.5,1.,2.,4.,8.,16.,32.,48.,64.
r_e (Water cloud)	4., 7., 9., 11., 14., 17., 22., 30., 38., 46., 54., 62.
r_e (Ice cloud)	5.,10.,20.,40.,60.,80.,100.,110.,120.,130.,140.,150. (tentative)

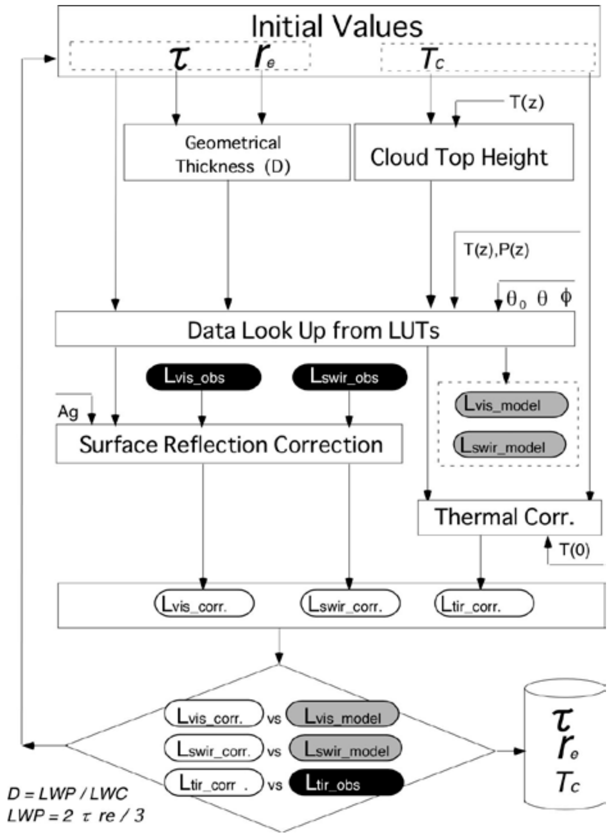

Fig. 2 Flow chart of the CAPCOM

3. Physical and Mathematical aspects of the CAPCOM

The solar reflectance method utilizes non-absorbing visible (Vis) and water-absorbing short-wave infrared (SWIR) wavelengths, such as 1.6, 2.2 and 3.7 μm, for the simultaneous retrieval of the cloud optical thickness at the 0.5μm wavelength and the effective particle radius. In this paper, we mainly discuss the solar reflectance method making use of SGLI Band 14 (1.05 μm), 16 (1.6 μm) and/or 17(2.2 mm), and 8 (10.8 μm). The effective particle radius of the clouds (r_e) is defined by

$$r_e \equiv \frac{\int_0^\infty r^3 n(r) dr}{\int_0^\infty r^2 n(r) dr}, \qquad (1)$$

where $n(r)$ is the number size distribution as a function of the particle radius *r*. We used a log-normal size distribution in the calculations,

$$n(r) = \frac{c}{r} \exp\left[-\frac{(\ln r - \ln r_0)^2}{2\sigma^2} \right], \qquad (2)$$

where *c* is a constant, r_0 is the mode radius, which is related to the effective particle radius as $r_e = r_0 e^{2.5\sigma^2}$, and σ is the log-standard deviation of the size distribution. Here, $\sigma = 0.35$ was assumed for marine stratocumulus clouds in our analyses. For the satellite signal simulation, we used an accurate and efficient radiative transfer scheme (Nakajima and Tanaka 1986, 1988) extended to include the thermal radiative transfer (Stamnes et al. 1988). We assumed a Lambert surface for the underlying surface. This assumption will not introduce a significant error in the analyses if we use an equivalent flux albedo for cloudy atmospheres (Nakajima et al. 1991)

We retrieved τ_c at the 0.5-μm wavelength and r_e from SGLI Band 14 and 16(and/or 17) on the basis of the fact that Band 14 and 16 (17) primarily depend on the cloud optical thickness and the effective particle radius, respectively. Although the concept of the retrieval is simple, some difficulties occur when determining the cloud properties from the measured SGLI spectral radiance. It is necessary to remove the unexpected radiation components (e.g. solar radiation reflected by the ground) from the observed radiance.

4 Formulations of the radiative components

According to the radiative transfer theory for parallel plane layers with an underlying Lambert surface, we remove the unexpected radiation components, such as the solar radiation reflected by the ground surface and the thermal radiation emitted from the cloud layer and the ground surface, from the satellite-received radiance, L_{obs}, in order to decouple the radiation component reflected by the cloud layer, L, as follows:

$$
\begin{aligned}
&L(Z_c, D_c, \tau_c, r_e; \mu, \mu_0, \phi) \\
&= L_{obs}(Z_c, D_c, \tau_c, r_e; \mu, \mu_0, \phi) \\
&-t(Z_c, D_c, \tau_c, r_e; \mu)\frac{A_g}{1-\bar{r}(Z_c, D_c, \tau_c, r_e)A_g}\, t(Z_c, D_c, \tau_c, r_e; \mu_0)\frac{\mu_0 F_0}{\pi}
\end{aligned}
\qquad (3)
$$

where F_0 is the extraterrestrial solar flux, and τ_c and τ_u are the optical thicknesses of the cloud layer, and the atmosphere above the cloud layer, respectively. μ_0 and μ are the cosines of the solar and satellite zenith angles, respectively, ϕ is the azimuthal angle of the satellite relative to the sun. Z_c and D_c are the top height and the geometrical thickness of the cloud, respectively.

The transmissivity t, the plane albedo r, and the spherical albedo $\bar{r}$ are given by

$$
\begin{aligned}
&t(\tau_c, r_e; \mu_0) \\
&= \frac{1}{\pi}\int_0^{2\pi}\int_0^1 T(\tau_c, r_e; \mu, \mu_0, \phi)\mu d\mu d\phi + e^{-\tau/\mu_0}
\end{aligned}
\qquad (4)
$$

$$r(\tau_c, r_e; \mu) = \frac{1}{\pi} \int_0^{2\pi} \int_0^1 R(\tau_c, r_e; \mu', \mu, \phi) \mu' \, d\mu' \, d\phi \tag{5}$$

$$\bar{r}(\tau_c, r_e) = 2 \int_0^1 r(\tau_c, r_e; \mu) \mu d\mu, \tag{6}$$

where $T(\tau_c, r_e; \mu, \mu_0, \phi)$ and $R(\tau_c, r_e; \mu', \mu, \phi)$ are bi-directional transmission and reflection functions respectively. The second term in Eq. (3) is ground-reflected radiation components Multiple reflections between the ground surface and the upper layer are taken into consideration in Eqs. (3). However, this effect is sufficiently small to regard $\bar{r}(\tau_c, r_e) A_g$ as almost zero, especially for optically thin clouds and ground surfaces with low reflectance. On the contrary, with optically thick clouds and large ground albedo, this effect is relatively large at visible wavelengths since the large cloud spherical albedo reflects radiation from the ground surface, while the relatively large transmissivity allows this radiation component to be transmitted into space. These formulations are exact when we consider monochromatic radiance. We further introduce a process of averaging of the variables in the formulations with respect to the wavelength. For example, t is averaged with a sub-channel response function of SGLI as

$$t = \sum_{\mathrm{n=1}}^{\mathrm{N}} \varphi_{\mathrm{n}} \left\{ \sum_{\mathrm{k=1}}^{\mathrm{M}} \left(\xi_{\mathrm{n,k}} \times t_{\mathrm{n,k}} \right) \right\} / \sum_{\mathrm{v=1}}^{\mathrm{n}} \varphi_{\mathrm{n}} \, , \tag{5}$$

where φ_{n} is the response function of the n-*th* subchannel wavelength for each SGLI Band, $\xi_{\mathrm{n,k}}$ is the weight of the k-*th* k-distribution, and $t_{n,k}$ is the transmissivity for the k-*th* k-distribution at the n-*th* wavelength. This averaging process, which was applied to Eqs. (3) introduces a non-negligible error into the case of thin cloud layers in which the spectral variation of $t_{n,k}$ becomes large. However, in most cases in which this process is applied, the error remains small, and it is possible to estimate the undesirable radiation components in Eqs. (3) by using spectrally averaged variables for each channel.

Reference:

[1]. Nakajima, T. Y., and T. Nakajima, 1995: Wide-area determination of cloud microphysical properties from NOAA AVHRR measurements for FIRE and ASTEX regions. Journal of the Atmospheric Sciences, 52, 4043-4059.

[2]. Kawamoto, K., T. Nakajima, and T. Y. Nakajima, 2001: A global determination of cloud microphysics with AVHRR remote sensing. Journal of Climate, 14, 2054-2068.

[3]. Stamnes, K., Tsay, S. -C., Wiscombe, W. J., & Jayaweera, K. (1988). Numerically stable algorithm for discrete-ordinate-method radiative transfer in multiple scattering and emitting layered media. Applied Op- tics, 27(12), 2502–2509.

[4]. Nakajima, T. et al. Determination of the optical thickness and effective particle radius of clouds from reflected solar radiation measurements. Part II. Marine stratocumulus observations. J. Atmos. Sci. 48, 728–750, 1991.